A New Imaging Model*

Manoj Aggarwal Narendra Ahuja
University of Illinois at Urbana-Champaign
405 N. Mathews Ave, Urbana, IL 61801
{manoj,ahuja}@vision.ai.uiuc.edu

Abstract

This paper has been prompted by observations of some anomalies in the performance of the standard imaging models (pin-hole, thin-lens and Gaussian thick-lens), in the context of composing omnifocus images and estimating depth maps from a sequence of images. A closer examination of the models revealed that they assume a position of the aperture that conflicts with the designs of many available lenses. We have shown in this paper that the imaging geometry and photometric properties of an image are significantly influenced by the position of the aperture. This is confirmed by the discrepancies between observed mappings and those predicted by the models. We have therefore concluded that the current imaging models do not adequately represent practical imaging systems. We have proposed a new imaging model which overcomes these deficiencies and have given the associated mappings. The impact of this model on some common imaging scenarios is described, along with experimental verification of the better performance of the model on three real lenses.

1. Introduction

This paper has been prompted by observations of some anomalies in the performance of the standard models of image formation. Imaging models describe geometric and photometric mappings between a scene and its image on a sensor. The three imaging models commonly used in computer vision are the pin-hole, thin-lens and the Gaussian thick-lens models. We recently investigated these models in the context of composing omnifocus images and estimating depth maps from a sequence of images. These processes involved selection of pixels from different images and their compilation into new images; they thus intensely exercised the models' abilities to predict imaging parameters, and revealed the inadequacies of all three models to correctly predict the geometric and photometric mappings. We have since developed an alternate model that overcomes these deficiencies and is the subject of this paper.

We first briefly review the three imaging models before presenting their deficiencies. The pin-hole model represents an imaging system by a point aperture placed between the scene and the sensor, and the image location of a scene point is given by the intersection of sensor plane with the line joining the scene point and the point aperture. This simple model is parameterized by the distance v of the location of the aperture from the sensor.

The thin-lens model is an improvement over the pin-hole model. It represents an imaging system in terms of an ideal thin lens with finite aperture. This model is parameterized by the focal length F of the lens, and the distance v of the lens center C from the sensor. The thin-lens model has the same geometric mapping as the pin-hole model, but it also attempts to capture photometric effects including sharpness of the acquired image and light accumulation over a finite aperture that are unaccounted for in the pin-hole model.

An imaging lens typically is not a single lens, but a combination of multiple lenses having finite thickness, and a Gaussian thick-lens model [5, 7] has been proposed in literature for this case. This model represents a lens by two equivalent refracting surfaces called principal planes. The sensor position v in this model is measured with respect to one of the principal planes and the object distance u is measured with respect to the other.

We briefly describe the experiment in which the observed mappings between the scene and its images were found to be in conflict with the traditional models. The experiment was in the context of composing omnifocus images [2] and estimating depth map from multiple images acquired at different positions of the sensor [3, 8]. According to the three models, if the sensor is shifted by δv, the parameter v (v_{new}) of the new configura-

*The authors gratefully acknowlege the support of a grant from Advanced Telecommunication Research International, Japan

0-7695-1143-0/01 $10.00 © 2001 IEEE

tion is given by $v_{new} = v + \delta v$, since the lens itself is unaltered. Thus, the magnification between the two positions is given by $\frac{v+\delta v}{v}$. In spite of precise calibration and precise knowledge of δv's, the observed magnification values were quite different from those computed using the models. The unexplained result of this experiment led us to closely examine the three models and various assumptions made by them.

We have concluded that the aforementioned discrepancies were in part due to shortcomings in the traditional models of image formation. This paper describes these shortcomings and proposes an alternative model. We show that the Gaussian thick-lens and the simpler models do not realistically account for the effect of the aperture on the imaging process. It assumes a position of the aperture that simplifies the model but conflicts with the designs of many available lenses. From the imaging geometry it is clear that the position of the aperture plays a significant role in determining the geometric and photometric mapping performed by the lens. For instance, it is well known that if the aperture is relocated to the front focal plane the camera becomes telecentric, while the Gaussian model for the new configuration is unchanged. Therefore, the assumptions related to the aperture have a direct impact on the validity of the traditional imaging models. We propose a new imaging model for isotropic lenses that explicitly involves the dependence on aperture and includes the Gaussian model as a special case.

Section 2 presents additional relevant aspects of the Gaussian thick-lens model and qualitatively describes the impact of the assumption related to the position of the aperture. Section 3 describes the proposed imaging model, presents the geometric and photometric mappings represented by the model, and illustrates their significance in common imaging situations. In Section 4, we present two sets of experiments on two fixed focal length lenses and one zoom lens to compare the performance of the proposed and the Gaussian models. Section 5 presents concluding remarks.

2. The Gaussian thick-lens model

Gauss had postulated that any lens can be modeled using two equivalent refracting planes, called principal planes. The points of intersections of the principal planes with the optical axis are called principal points and are denoted by P_1 and P_2. The focal length F is defined as the distance between P_2 and F_2, where F_2 refers to the focal point where rays parallel to optical axis converge after refraction. There are two additional points N_1 and N_2 called nodal points that characterize this model. This pair has the property that a paraxial ray passing through one of them emerges from the other at the same slope. For a lens in air, the points N_1 and N_2 coincide with P_1 and P_2.

Let u denote the distance along the optical axis between a point object and the principal point P_1, and v' denote the perpendicular distance between the focused image and point P_2. Then, it can be shown [7] that u, v', F satisfy the lens law given by $\frac{1}{F} = \frac{1}{u} + \frac{1}{v'}$. The distances u and v are said to be *conjugate* if they satisfy the lens law.

We briefly describe the geometric and photometric mappings according to the Gaussian model. Consider an imaging configuration shown in Fig. 1. We denote the coordinates of a point object O as (x_o, y_o, z_o), with respect to an orthogonal coordinate system called lens coordinate system (LCS) located at the first principal point with z-axis along the optical axis and pointing towards the sensor. If the sensor is conjugate to the object, then the image of object O is a point I'. However, in general, image I of a point is defocused and appears as a circularly symmetric blob (assuming circular aperture), whose center according to the Gaussian model is given by the intersection of ray OP_1 after refraction and the sensor. Thus, we refer to the coordinates of I to be those of its center. We define a image coordinate system ICS located at the principal center (point of intersection of optical axis with sensor) with x and y coordinates spanning the sensor plane. Let the distance between the sensor and the second principal plane be v, then the coordinates of I are given by

$$\begin{aligned} I &= \left(\frac{\alpha x_o}{S_x}, \frac{\alpha y_o}{S_y}, 0\right) \quad \text{in ICS, where,} \\ \alpha &= \frac{v}{z_o}, \end{aligned}$$

and S_x and S_y are the scale factors along the horizontal and vertical scanning directions of the sensor.

With regard to the photometric properties, the relationship between the scene radiance and image irradiance E has been derived by Horn [6], and is given by

$$E = L\left(\frac{A}{v^2}\right)\cos^4 w, \tag{1}$$

where w is the angle made by ray OP_1 with the optical axis, A is area of the aperture and L is the radiance of object O in the direction $O\vec{P}_1$. The analysis assumes that the aperture is located at the first principal plane. Again, as in the case of geometric mapping, the orientation of the ray OP_1 with respect to the optical axis plays a central role in determining the photometric properties of the image of point O.

The geometric and photometric mappings for a thin-lens also have the same form as those for the Gaussian model, which suggests that the Gaussian and the

simpler models might be related. This is indeed the case and it can be shown that the Gaussian model reduces to a thin-lens model. Qualitatively, the reduction of the Gaussian model to the simpler models can be explained as follows. The two principal planes in the Gaussian model are unit magnification images of each other [7], which means every ray that enters the first principal plane emerges from the other at the same height. Thus, the Gaussian model can be simplified by collapsing the second principal plane with the first principal plane and measuring all distances with respect to the joint planes. Both the Gaussian model with collapsed principal planes and the thin-lens model follow the same lens law, and for a lens in air, a ray through P_1 emerges through P_2 with the same slope. This implies that the geometric and photometric mapping represented by the Gaussian model can be equivalently modeled with a thin lens placed at the first principal plane and the sensor at a distance v from the thin-lens. Further, since a thin-lens model is geometrically equivalent to a pin-hole model with a thin-lens replaced by a pin-hole aperture, Gaussian model is geometrically equivalent to a pin-hole model as well.

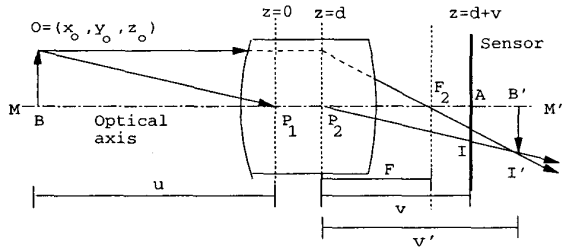

Figure 1. Imaging geometry for Gaussian model.

2.1. Assumption about the aperture in Gaussian model

In the previous section, we had noted that within the Gaussian model the geometric and photometric mappings between an object point O and its image are determined by the ray OP_1. The strong dependence on the first principal point results from an implicit assumption that the effect of aperture (position and size) in a lens system can be modeled by an *equivalent aperture* located at the first principal plane [6]. In this section, we will first explain why this assumption is not valid for real lenses, and then demonstrate the influence of aperture location on the geometric and photometric mapping in an imaging system which is unaccounted for in the Gaussian model.

In an imaging system, the cone of light rays from an object point which is eventually refracted to the sensor

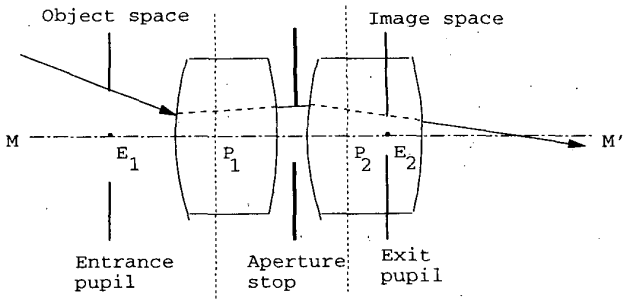

Figure 2. Entrance and Exit pupil

is determined by the shape, size and the location of the aperture. If the aperture is outside the lens (as in Fig. 3), this cone of light can be readily determined. However, in most lenses(Fig. 2), the physical aperture is between the multiple lens elements and the incident cone of light rays reaches the aperture after multiple refractions through the set of lens elements between the object and aperture. The incident cone of light can then be seen as constrained by an equivalent aperture on the object side. This equivalent aperture as seen by all objects is given by the conjugate image of the physical aperture through the lens elements between the physical aperture and the scene, and is called *entrance pupil* [7]. Similarly, *exit pupil* is defined as the image of the physical aperture formed by the lens elements on the image side [7]. The cone of light rays received at every sensor element thus appears to come from the exit pupil, in the same manner as all incident light rays intercepted by the lens appear to originate at the entrance pupil.

Contrary to the assumption made by the Gaussian model, the entrance pupil (which may be considered as the equivalent aperture used in the Gaussian model) does not necessarily coincide with the first principal plane. For instance, if the physical aperture is in front of the lens, the entrance pupil coincides with the physical aperture irrespective of the lens or the distance of the aperture from the lens. However, in most lenses, the aperture is located between lens elements. The displacement between the entrance pupil and first principal plane for seven such lenses is tabulated in Table 1. The parameters were obtained using a calibration technique whose description has been omitted for the lack of space. In fact, the displacement is non-zero for most of the CCTV lenses from Tamron, Cosmicar, Fujinon, Navitar and JML Optical that we have experimented with. We next examine the influence of such a displacement on the imaging process.

Lens	E_1	E_2	P_1	F, P_2	a
23FM16	26.03	44.53	15.70	16.28	10.33
23FM25	7.87	19.59	14.88	25.00	-6.91
C31630	30.34	44.37	20.05	16.20	10.29
C22525	30.27	30.81	25.59	25.00	5.21
DO1614	25.53	65.28	13.45	16.00	12.07
DO2514	27.43	16.68	39.91	25.00	-12.48
V18x6	121.53	430	104.28	18	17.25
V18x6	15.53	430	-43.07	70	58.60

Table 1. Model parameters of some commercially available lenses. All distances are in mm and are with respect to the focal point.

2.2. Impact of incorrect modeling of aperture in Gaussian model

Consider an imaging configuration shown in Fig. 3. It shows a lens system represented as a thin-lens obtained by collapsing the two principal planes and a physical aperture at a non-zero distance from the lens. Let O be a point object in the object plane and a sensor at a position which in general is not conjugate to the object. In this case, the rays from an object point O converge ahead of the sensor and then intercept the sensor over a finite non-zero area. Therefore, depending on the shape and location of the aperture, the object O illuminates different sub-regions of the sensor. Consequently, both geometric and photometric properties of the image depend on aperture shape and position and cannot be correctly modeled by an equivalent aperture placed at the lens center. In fact, if the aperture were placed at the front focal plane, the imaging system would be telecentric [7, 11], and as a result image magnification would be independent of sensor position; this effect cannot be explained based on the Gaussian or the thin-lens model.

The aforementioned imaging configuration demonstrates that the effect of the aperture cannot be modeled by assuming an equivalent aperture at the first principal plane. Consequently, the Gaussian thick-lens model does not hold for many common imaging situations. In the next section, we will present a model which takes into account the non-zero displacement between the entrance pupil and the first principal plane.

3. Proposed Imaging Model

We define our new model to consist of the two principal planes, the focal point, and the entrance and exit pupils. We also define two points E_1 and E_2 which are the intersections of the entrance and the exit pupils with the optical axis, respectively. The points E_1, E_2,

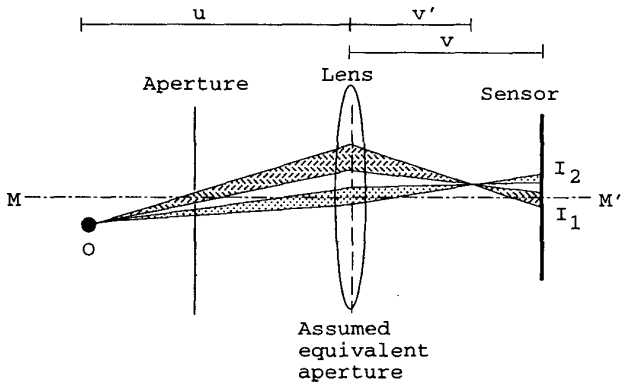

Figure 3. Role of aperture in an imaging system.

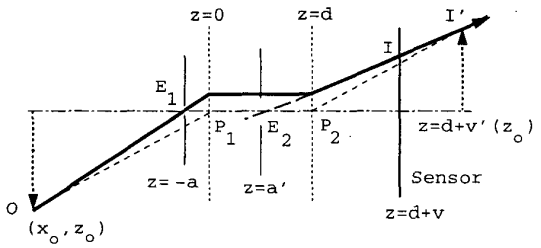

Figure 4. Imaging geometry for proposed model.

P_1 and P_2 in general are all distinct. In the next two sections, we will derive the geometric and the photometric mappings between the scene and its image according to the proposed model.

3.1. Imaging geometry

Consider an imaging configuration shown in Fig. 4. We define the ray from an object point O that passes through the center (centroid) of the aperture as the *principal ray*. For isotropic lenses, with an aperture whose center is on the optical axis, the principal ray is given by OE_1. As noted in Section 2.1, the image of a scene point is determined by the cone of rays from point O that are allowed to pass through the lens. In general, the cone of light from point O will impinge the sensor over a finite area, i.e. the image is defocused and appears like a blob, unless O is conjugate to the sensor, in which case the image is a point. The principal ray by definition forms the medial axis of the light cone, and hence the center of the blob will correspond to the intersection of principal ray with the sensor. Thus according to the proposed model, the underlying geometry of the image is determined by the principal ray.

Let the sensor be located at a distance v from the second principal plane along the optical axis. Since,

the underlying geometry is determined by the center of the blob, we refer to the coordinates of I to be those of its center. The coordinates of I, i.e. the point of intersection of the principal ray and the sensor can be derived to be

$$I = \left(\frac{\alpha x_o}{S_x}, \frac{\alpha y_o}{S_y}, 0\right) \text{ in ICS, where,}$$
$$\alpha = \frac{1}{z_o + a}\left(v + a - \frac{va}{F}\right). \quad (2)$$

Under the transformations

$$\tilde{z}_o = z_o + a, \quad \text{and} \quad (3)$$
$$\tilde{v} = v + a - \frac{va}{F}, \quad (4)$$

the term α can be conveniently expressed as

$$\alpha = \frac{\tilde{v}}{\tilde{z}_o}, \quad (5)$$

which is the familiar expression for pin-hole perspective projection for a frontal planar sensor. This implies that the proposed model for an imaging system with a frontal sensor and fixed imaging parameters is geometrically equivalent to a pin-hole model with the following parameters: the pin-hole is located at the center of the entrance pupil E_1 and the distance of the sensor plane from the pin-hole is $\tilde{v}$.

The equivalent pin-hole model parameters will in general be different for two distinct[1] lenses even with same focal lengths, because the relative positions of the two pupils and the two principal planes in the two lenses could be different. Further, adjusting the focal setting on the lens to alter v also changes the parameters of the proposed model and hence the equivalent pin-hole model. For example, if we shift the sensor by δv it does not imply that the equivalent pin-hole image surface shifts by the same amount. In fact, from the definition of $\tilde{v}$ in equation (4) it follows that the equivalent shift $\delta\tilde{v}$ is given by

$$\delta\tilde{v} = \delta v\left(1 - \frac{a}{F}\right). \quad (6)$$

We note, the ratio $\frac{a}{F}$ is different for different lenses and determines the extent of departure of the traditional models from the proposed model.

Impact: To develop a sense for the errors that accompany the use of the simpler models, consider the usual imaging situation where images of a scene are acquired to focus on different objects at different locations. We use the magnification factor between two images obtained at sensor positions $v = 16.83$ and $v = 17.83$ with a Tamron 23FM16 lens (Table 1), as a measure for comparing the performances of the pin-hole and Gaussian model to the proposed model.

In Section 2, we had shown that the Gaussian model is geometrically equivalent to the pin-hole model. If that holds, a natural question that arises is why compare the performances of both the Gaussian and pin-hole model and why the analysis for any either case alone will not suffice? The answer is, it depends on the calibration method used to estimate the parameters of the two models. If the parameters of the pin-hole model are derived entirely from the Gaussian model, then the two models as proved in Section 2 are geometrically identical. However, if the pin-hole is estimated directly without first estimating the Gaussian model as in techniques proposed by Faugeras [4], Triggs [9], Tsai [10] and Zhang [12][2], the resulting parameters may in general be different. Further, in certain variations of these general calibration methods, some parameters of the pin-hole model are pre-constrained to assume known values from the Gaussian model. Depending on what assumptions are made, the estimated pin-hole model parameters and hence the consequent errors in the geometric mapping are different. We will compare the proposed, Gaussian and the two common variants of pin-hole models in the rest of this section. In this discussion we have assumed that the proposed model correctly represents the true imaging process, which has been experimentally verified later in Section 4.

Case 1. Pin-hole model estimated with no assumptions
Since no assumption are made, the estimated parameters $\tilde{v}$, $\tilde{S}_x$ and $\tilde{S}_y$, would be ideally identical to those of the equivalent pin-hole model (derived from the proposed model) and are given by $\tilde{v} = v + a - va/F = 16.48$mm, $\tilde{S}_x = S_x$ and $\tilde{S}_y = S_y$. If there is 1mm change in the sensor position and it is assumed that the pin-hole parameter $\tilde{v}$ also changes by 1mm, then the predicted magnification is $(16.48 + 1)/16.48 = 1.0607$.

Case 2. Pin-hole model estimated with assumption $\tilde{v} = v$
Irrespective of the estimated scale parameters, the image magnification is given by $(16.83+1)/16.83 = 1.0594$.

Case 3. Gaussian model
In the Gaussian model, it is assumed that $a = 0$, which implies $\tilde{v} = v$. Thus, the predicted magnification is given by $(16.83 + 1)/16.83 = 1.0594$.

Case 4. Proposed model
The proposed model however predicts the magnification to be $\frac{\tilde{v}+\delta\tilde{v}}{\tilde{v}}$ which evaluates to $(16.48 + 0.365)/16.48 = 1.0221$.

[1] We define two lenses to be distinct if their lens prescriptions are different.

[2] Refer to Zhang's paper for a thorough list of references on camera calibration

Consider a pixel with coordinates (200,200) w.r.t image center. The four cases would predict that this pixel will shift to locations (212.1,212.1), (211.9, 211.9), (211.9, 211.9), and (204.4, 204.4), respectively, in the new image. The resulting error of 7-8 pixels could be intolerable in many applications. We note that if in cases 1 and 2, the pin-hole parameters had been independently estimated for both configurations (i.e. without assuming $\tilde{v_2} = \tilde{v_1} + 1$), then the estimated values of $\tilde{v_1}$ and $\tilde{v_2}$ would have been identical to those determined by the proposed model, resulting in a common estimate for image magnification. Even though estimating the parameters individually for all possible camera configurations would give the same results as the proposed model, it is an impractical approach and it defeats the purpose of modeling and calibration.

3.2. Photometric properties

The relationship between the radiance of an object point and the irradiance E at the corresponding point on the sensor, can be derived to be

$$E = L\left(\frac{\tilde{A}}{\tilde{v}^2}\right)\cos^4\beta, \tag{7}$$

where β is the angle made by ray OE_1 with the optical axis, $\tilde{A}$ is the area of the entrance pupil and L is the radiance of object O in the direction $\vec{OE_1}$. The spatial variation in irradiance is in the familiar $\cos^4$ form, however, the angle β is defined by the center of entrance pupil, and not by the first principal point as done in the Gaussian model. Note that the expression for irradiance in equation (7) is identical to that for a thin lens of aperture size $\tilde{A}$ placed at position $z = -a$ in LCS, with the sensor at a distance $\tilde{v}$ from the thin lens. Therefore, such a thin-lens would correctly model the photometric response of the imaging system. The geometric mapping performed by this thin-lens model is identical to that of a pin-hole model with the pin-hole at the location of the thin-lens. Further, we had shown in Section 3.1 that the pin-hole model which captures the geometric mapping predicted by the proposed model for the given imaging configuration places the pin-hole and the sensor at the same locations as in the aforementioned photometric case. As the final result, the aforementioned thin-lens model exactly represents both the geometric and photometric mappings performed but they are valid for a particular configuration of the imaging system.

As imaging configuration, e.g., the focus setting v, changes, the parameters of the equivalent thin-lens model change as well. The parameters of the new configuration can be determined using the transformation equations (3,4).

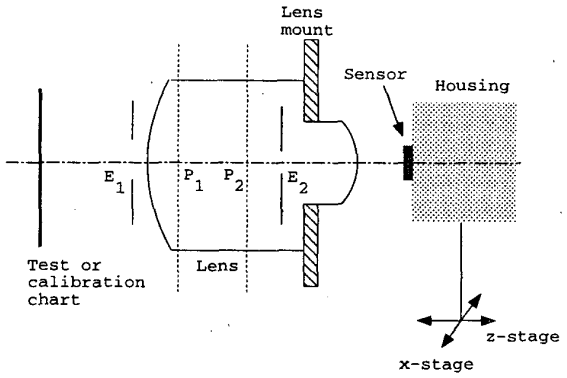

Figure 5. Experimental setup

4. Experiments

As we had shown in previous section, the proposed model always reduces to the thin-lens model when the parameters such as the thin-lens location and its distance to the sensor are chosen as determined by the transformation equations (3,4). In the experiments, we present in this section, we compare the accuracy of the *relationship* between the camera configuration and the parameters of the thin-lens models, as predicted by the Gaussian and the proposed models. This relationship for the proposed model is given by the transformation equations (3,4), while for the Gaussian model is as described in Section 2. We present two experiments to compare the accuracy of the relationship for the cases of proposed and the Gaussian models. The two experiments involve comparing the image magnification and intensity variation due an axial shift in the sensor position as predicted by the proposed and the Gaussian model to the observed value.

Consider the experimental setup shown in Fig. 5. For all our experiments we used a modified Pulnix TM720 CCD camera. The camera was split into two parts, the lens mount and the camera housing containing the electronics and the CCD sensor. The housing was mounted onto a three degrees of freedom calibrated stage for positioning the sensor.

Experiment 1: Image magnification due to a known change in focus setting. A planar chart consisting of a regular grid of dots was placed at the distance of 400mm from the front surface of the lens mount and multiple images of the chart were acquired for a range of z-stage settings. We identified pairs of equidistant points on the chart, and in each image measured the average value of the separation between the points in the identified pairs. The average distance values were then normalized by dividing by the minimum

average distance which corresponds to that of the closest sensor position. The normalized value thus measures the magnification in the image obtained at corresponding z setting, compared to that in the image obtained at the smallest z setting.

The experiment specific setup involved the following. We aligned the sensor center to the optical center (C_x, C_y) using the technique described in [1]. The focus ring on the lens was set to infinity, f-number was set to the smallest value, and the z-stage was adjusted to focus on a far away object. This z-setting was used as the reference $z = 0$.

The experiment was performed for three lenses: Tamron 23FM16, Tamron 23FM25 and Canon Zoom Lens V6x18, for zoom setting 18mm. Fig. 6 shows the normalized values of the average image plane distance ('x' marks) as a function of sensor position z. As expected, the image size changes linearly with sensor position. We will refer to the graph of image size as a function of sensor position as the magnification curve, and its (constant) slope as the magnification rate. Fig. 6 also shows the magnification curves as predicted by the Gaussian and proposed models. The $\tilde{v}$ parameter of the corresponding equivalent thin-lens models were used, after normalization, to plot the predicted magnification curves. The $\tilde{v}$ parameter for the equivalent pinhole model derived from the Gaussian model is given by $\tilde{v} = v = F + z$, while for the proposed model is a given by $\tilde{v} = v + a + va/F$. It can be seen that the magnification curves predicted by the proposed model match very closely with the observed variation for each of the three lenses, while the Gaussian magnification curves exhibit a significant departure.

Experiment 2: Photometric variation with sensor position. This experiment is similar to the first experiment except that intensity variation instead of image magnification was analyzed as a function of sensor position. We used a white sheet of paper as the scene and acquired images for a range of sensor positions. We also acquired an image with the lens covered, which we refer to as the dark image. We subtracted the dark image from the images of the white sheet and plotted the intensity of the central pixel as a function of the sensor position. Fig. 7 shows the plots for the three lenses: Tamron 23FM16, Tamron 23FM25 and Canon V6x18 for zoom setting 18mm. The maximum intensity value in each plot was normalized to 1 by dividing it by the intensity value observed at the closest sensor position. Fig. 7 also shows the plots of photometric variation predicted by the Gaussian and proposed models. As in the previous experiment, the proposed model matches the observation better than the Gaussian model for all three lenses.

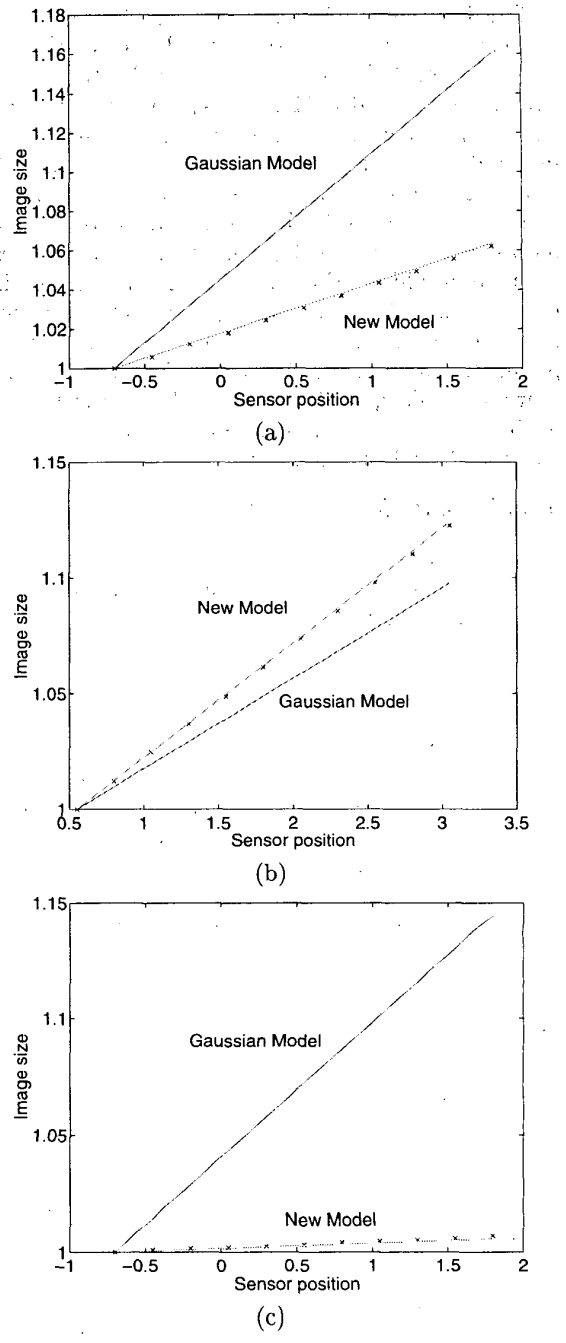

Figure 6. Plot of distance between two image points as a function of sensor position. The sensor position is in reference to position where infinity is in focus. (a) Tamron 16mm lens (23FM16), (b) Tamron 25mm lens (23FM25), and (c) Canon V6x18, zoom setting 18mm

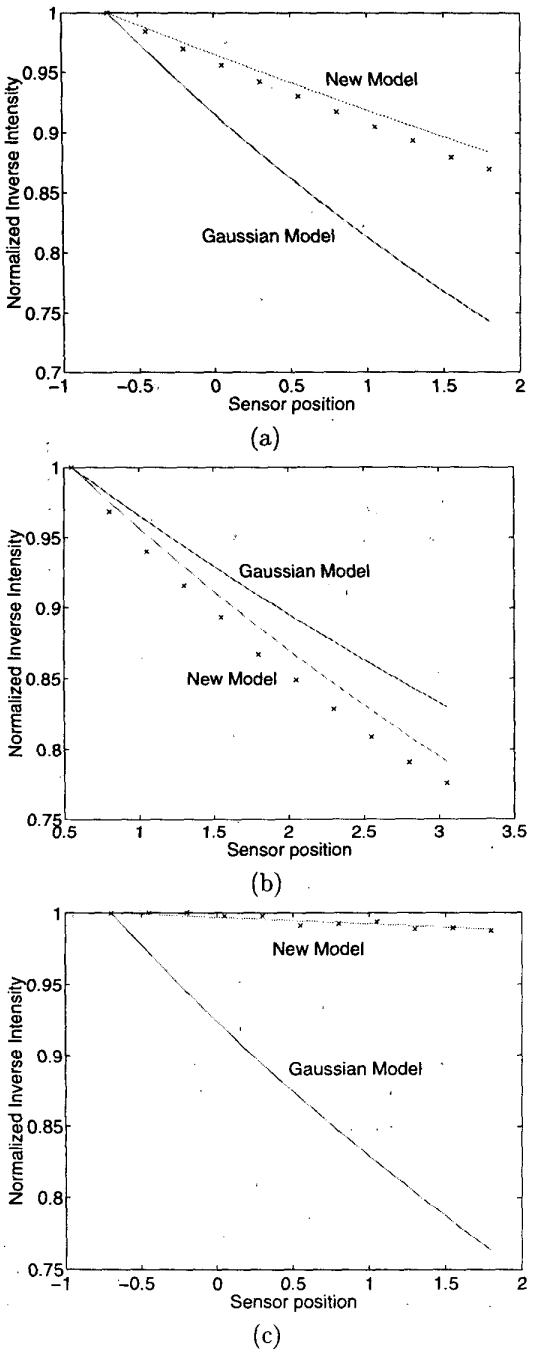

Figure 7. Plot of normalized intensity at the image center as a function of sensor position. The sensor position is in reference to position where infinity is in focus. (a) Tamron 16mm lens (23FM16), (b) Tamron 25mm lens (23FM25), and (c) Canon V6x18, *zoom* setting 18mm.

5. Conclusions

We have presented a new imaging model which accounts for the position and size of the physical aperture along with the multiplicity and finite thickness of lens elements in commonly used imaging lenses. The position and size of the aperture plays a critical role in determining the geometric and the photometric mapping between the scene and its image. The proposed imaging model has been compared with the conventional Gaussian thick-lens model and the common assumption of a fixed equivalent aperture (entrance pupil) coincident with the first principal plane, irrespective of the location of the physical aperture, has been critically evaluated.

References

[1] M. Aggarwal and N. Ahuja. Camera center estimation. In *International Conference on Pattern Recognition*, pages 876–880, September 2000.

[2] P. J. Burt and R. J. Kolczynski. Enhanced image capture through fusion. In *International Conference on Computer Vision*, pages 173–182, 1993.

[3] J. Ens and P. Lawrence. An investigation of methods for determining depth from focus. *IEEE Transactions on Pattern Analysis and Machine Intelligence*, 15(2):97–107, February 1993.

[4] O. Faugeras. *Three-dimensional Computer Vision: A Geometric Approach.* MIT Press, 1996.

[5] E. Hecht and A. Zajac. *Optics.* Addison Wesley, 1974.

[6] B. K. P. Horn. *Robot Vision.* The MIT Press, Cambridge, Mass., 1986.

[7] R. Kingslake. *Optical System Design.* Academic Press, 1983.

[8] M. Subbarao. Accurate recovery of three-dimensional shape from image focus. *IEEE Transactions on Pattern Analysis and Machine Intelligence*, 17(3):266–274, March 1995.

[9] B. Triggs. Autocalibration from planar scenes. In *European Conference on Computer Vision*, volume 1, pages 89–105, 1998.

[10] R. Y. Tsai. A versatile camera calibration technique for high-accuracy 3D machine vision metrology using off-the shelf TV cameras and lenses. *IEEE Journal of Robotics and Automation*, RA-3(4):323–344, August 1987.

[11] M. Watanabe and S. K. Nayar. Telecentric optics for focus analysis. *IEEE Transactions on Pattern Analysis and Machine Intelligence*, 19(12):1360–1365, December 1997.

[12] Z. Zhang. A flexible new technique for camera calibration. *IEEE Transactions on Pattern Analysis and Machine Intelligence*, 22(11):1330–1334, November 2000.